Acoustic satellites of helicon resonance

V. T. Petrashov

Institute of Solid State Physics, USSR Academy of Sciences

Helicon resonances in plane-parallel single-crystal plates of ultrapure indium were investigated experimentally. It was observed that besides the resonances described by the known theory [R. G. Chambers and B. K. Jones, Proc. Roy. Soc. (London) A270, 417 (1962); P. A. Penz, J. Appl. Phys. **38**, 4047 (1967)] there exist additional peaks whose resonant magnetic fields depend nonlinearly on the excitation frequency. These peaks can appear near a helicon resonance at both stronger and weaker magnetic fields. The spectrum of the flexural acoustic waves in a plate of ultrapure metal is calculated with account taken of the propagation of helicons in the plate, and it is shown that near the helicon resonance the acoustic characteristics change so strongly that acoustic resonances, whose positions agree with the experimentally observed ones, can occur when the magnetic field varies in a small range.

PACS numbers: 43.35.Rw, 76.90. + d

1. INTRODUCTION

This paper reports an experimental investigation of helicon resonances[1,2] in plane-parallel single-crystal plates of pure indium. It was observed that besides the resonances described by the unknown theory,[3] there exist additional resonance peaks. The aim of the paper is to elucidate the nature of these new resonance peaks.

The picture of helicon resonances in a thin (one dimension much smaller than the two others) plate in the case of symmetrical excitation is the simplest: the resonance should occur whenever the plate thickness spans an odd number of helicon half-waves. The values of the resonant frequencies ω_n can be obtained with the aid of the dispersion relation

$$k^2 = 4\pi |N_e - N_h| e\omega/cB \cos\theta \tag{1}$$

with account taken of the resonance condition

$$k = (2n+1)\pi/d, \quad n = 0, 1, 2 \dots . \tag{2}$$

Here k is the wave vector of the helicon, ω is the frequency, B is the external constant magnetic field, N_e and N_h are the concentrations of the electrons and holes, respectively, and θ is the angle between the field B and the wave propagation direction, which coincides with the normal to the plane of the surface.

After substituting (2) in (1) we obtain

$$\omega_n = (2n+1)^2 \pi c B_0 \cos\theta/4d^2 |N_e - N_h| e, \tag{3}$$

where B_0 is the magnetic field in which the resonance is observed.

Relation (3) expresses one of the most characteristic properties of helicon resonance, viz., the direct proportionality of the exciting frequency to the constant magnetic field under the resonance condition. The proportionality coefficient is determined only by the electronic characteristics of the metal and by the geometry of the experiment.

The picture becomes more complicated in thick plates, since the resonance condition is determined not by one dimension, as in (2), but in general by all three dimensions of the plate. It was established[4,5] that the resonant frequencies are well described in this case by equations of the type

$$\omega_{lmn} = \omega_0 \alpha_{lmn}; \quad l, m, n = 0, 1, 2, \dots, \tag{4}$$

where ω_0 is the resonant frequency of a thin, essentially infinite, plate (3), the coefficients α_{lmn} depend on the ratios of the transverse dimensions of the plate to the thickness, and on the numbers l, m, n, and do not depend on the magnetic field.

In the experiment, the decrease of the transverse dimensions of the plate leads to the onset of satellite resonances near the main resonances, close to the positions of ω_n calculated in accord with (3). These satellites, which are of the helicon type, should occur only on the higher-frequency side (when the resonances are plotted as functions of the frequency with constant B) or on the side of the weaker magnetic fields (at constant ω). The position of each satellite is such that at resonance the excitation frequency is proportional to the magnetic field.

We proceed now to report the experimental results.

2. EXPERIMENT

2.1 Samples, procedure, experimental conditions. The single-crystal samples were made from ultrapure indium with resistivity ration $\rho(300K/\rho(1.4K) = 2 \times 10^5$, obtained by the method of Ref. 6 from the Pure Ingredients Division of our Institute.

The samples were grown in a dismountable polished quartz mold and were plates measuring $1.5 \times 10 \times 50$ mm. The long axis of the sample coincided with the [110] axis, the [001] axis made an angle of 30° with the normal to the surface.

The method of crossed coils was used: the signal from an acoustic generator, of frequency 20–8000 Hz, was applied to the primary coil; the signal from the secondary coil was amplified and was registered, synchronously detected, and plotted with an *x-y* recorder. The coils covered an approximate volume $12 \times 12 \times 2$ mm. The measurements were made at a temperature 1.3 K, and the sample with its holder were placed directly in the helium.

The work was performed in an electromagnet capable of producing fields up to 20 kG with homogeneity not worse than 10^{-5} over the dimensions of the sample, and with a long-time stability not worse than 10^{-4}.

2.2 Experimental results. Figure 1a shows typical plots of the mutual inductance of the crossed coils against the magnetic field at various fixed frequencies. In weak magnetic fields this function had a simple form: a peak corresponding to the helicon resonance in our case with $n = 0$ under condition (2). The Hall constant $A_H = 1/|N_e - N_h|ec$, calculated from the position of this peak, turned out to be 1.6×10^{-12} $\Omega \cdot$cm $\cdot$G, which agreed within better than 1% with the known experimental values.[7]

With increasing excitation frequency, the resonance peak shifted towards stronger magnetic fields, its shape became initially distorted, and it split later into a number of resonant peak. When the resonance was recorded in fixed magnetic fields and the excitation frequency was smoothly varied, a similar picture was observed, Fig. 1b.

The reduction of the curves shows that the excitation frequency and the magnetic field remain directly proportional only for the peaks β(Fig. 1). The resonant peak for peaks of type α, located in weaker magnetic fields, and for peaks of type γ, located in stronger magnetic fields, depends nonlinearly on the excitation frequency (see also Fig. 7).
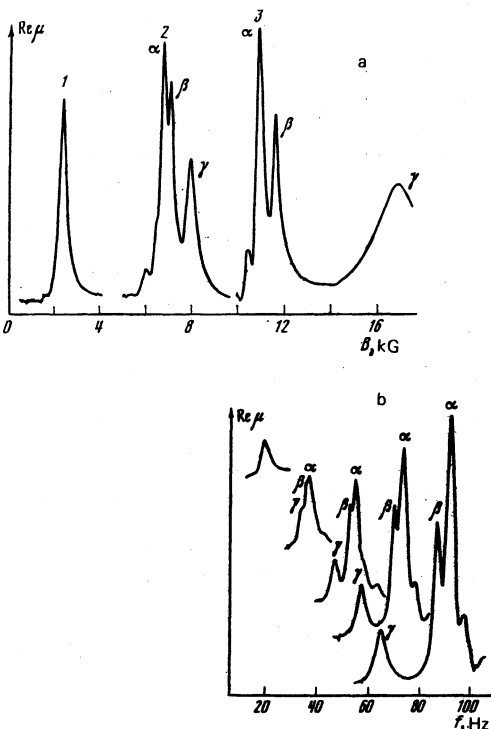
A discrepancy with the theory is thus observed at least at in two aspectse: first, a strong deviation from the proportionality of the excitation frequency to the resonant magnetic field; second, the appearance of a resonant peak in a field stronger than the helicon resonance at the same frequency.

It turned out later that when helicon resonances with higher numbers ($n = 1$, 2, 3) were excited in the sample under condition (2), there was no splitting of the resonant peak at all, Fig. 2.

In the subsequent experiments it turned out that the satellite resonances are quite sensitive to two factors: to the position of the coil system relative to the sample, and to the locations of the points were the sample was mounted (the sample was secured with small drops of BF-2 adhesive). The distance between the peaks β and γ decreased with increasing number of fastening points.

3. DISCUSSION OF RESULTS

The analysis of the results suggests that the observed satellite resonances are due to resonances of flexural acoustic waves, whose spectrum is strongly altered in the region of magnetic fields and frequencies at which helicon resonance sets in.

This is based on the following considerations. Consider a metal plate in a normal magnetic field, Fig. 3. Any flexure or rotation of the plate produces a tangential magnetic-field component that can subsequently propagate in the sample in the form of a helicon. Thus, the transverse flexural or rotational vibrations of the plate with frequency ω_n can lead to the onset of helicon resonance and are equivalent in a certain sense to the exciting-coil system.

On the other hand, the onset of helicon resonance leads to a resonant appearance of large magnetic moment of the plate, whose pondermotive interaction with the external magnetic field can cause rotation or flexure of the plate. Effects connected with such an interaction were first observed by Pippard and co-workers.[8]

A consistent solution of the problem of acoustic oscillations of a plate, with account taken of helicons propagating in it, can be broken up into several stages. We

FIG. 1. a) Dependence of the real part of the mutual inductance of crossed coils on the magnetic field at various fixed excitation frequencies: 1 – 22.1 Hz, 2 – 66.3 Hz, 3 – 110.5 Hz. b) Dependence of the real part of the mutual inductance of crossed coils on the excitation frequency in different fixed magnetic fields.
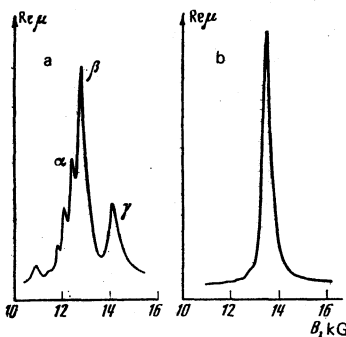

FIG. 2. Dependence of the real part of the mutual induction of crossed coils on the magnetic field at frequencies corresponding to excitation of helicon resonance with different numbers: a) $f = 132.6$ Hz, $n = 0$, b) $f = 1190$ Hz, $n = 1$.
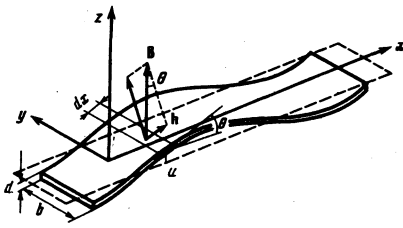
FIG. 3. Flexural oscillations of a plate in a magnetic field.

FIG. 4. Dependence of the propagation velocity of acoustic flexural waves in an indium plate placed in a magnetic field B = 9500 G. The dashed line shows the dependence in the absence of a magnetic field, and the dash-dot line the position of the helicon resonance (vertical line).

obtain first the magnetic moment M of an element dx of the plate, averaged over the sample thickness, at a helicon boundary condition set by the acoustic oscillations:

$$h(x, t) = B\theta(x, t),$$

where h is the tangential component of the external magnetic field, and θ is the angle between the external magnetic field and the normal to the surface of the plate, Fig. 3. We calculate next the pondermotive torque $K = M \times B$ and take it into account in the derivation of the wave equation for the flexural acoustic oscillations.

The calculation procedure is described in the Appendix (Item 2), and here we present the final form of the dispersion relation for the flexural oscillations of a plate placed in a magnetic field:

$$q^2 = \frac{\varkappa B^2 + [(\varkappa B^2)^2 + \frac{1}{3}\rho E d^2 \omega^2]^{1/2}}{\frac{1}{6} E d^2}, \tag{5}$$

where $\varkappa$ is the magnetic polarizability[9] of the plate, which in our case is given according to Ref. 3 by

$$\varkappa = \frac{1}{4\pi}\left(\frac{\text{tg}(kd/2)}{kd/2} - 1\right). \tag{6}$$

It is seen from the foregoing expressions that if the helicon damping is weak enough near the helicon resonance [see condition (2)] the acoustic characteristics of the plate undergo abrupt changes. Since (5) and (6) contain sufficiently well known quantities, it is easy to carry out the numerical calculations for our concrete case.

Figure 4 shows a typical plot of the propagation velocity c of the flexural acoustic oscillations, in an indium sample having parameters close to those used by us, in the absence of helicon damping. The plates behave as if it were much more rigid on the high-frequency side and has a decreased "effective" elasticity on the low-frequency side. The reason is that the elastic moments of the forces and the pondermotive moment are directed parallel at frequencies higher than the frequency of the helicon resonance, and antiparallel at lower frequencies.

Before we proceed to compare the theory with experiment, we make one more remark. At frequencies corresponding to long waves, when the wavelength greatly exceeds the sample length, i.e., at $qL \ll 1$ (L is the transverse dimension, the sample moves in essence as a rigid unit, and in this case we must solve the problem of the motion of the sample together with the sample holder and take into account the rigidity of the parts
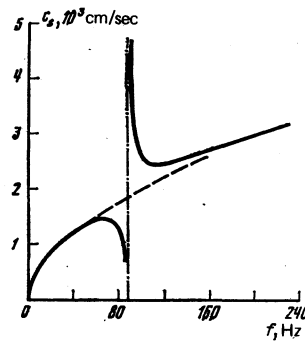
of the experimental setup. The solution of this problem is given in the Appendix (Item 1). We present some conclusions.

In the absence of a magnetic field, the natural frequencies of the oscillations of the sample holder with the samples are obtained from equations of the type

$$J^* \omega^2 - C^* = 0,$$

J^* is the effective moment of inertia, and C^* is the effective rigidity of the system.[10] As shown in the Appendix (Item 1), allowance for helicon propagation in the sample leads to a new resonance condition

$$-J^* \omega^2 + C^* = \varkappa B^2 V, \tag{7}$$

where V is the volume of the sample.

4. COMPARISON OF THEORY WITH EXPERIMENT

Acoustic resonances occur at definite wavelengths, such that the configuration of the plate oscillations satisfies the geometrical conditions of the experiment. The resonance condition can be written in the form

$$q = C, \tag{8}$$

where C is a certain constant determined by the geometry of the experiment. For example, for a hinge-supported plate 10 we have $C = \nu\pi/L$, $\nu = 1.2 \ldots$.

At a fixed frequency, resonance takes place in a field B_r that is obtained by solving the equation (5) for B with account taken of (6), (8), and (1). Such a problem can be solved, for example, graphically with the aid nomograms showing the dependence of q on the magnetic field (see Fig. 5). The position of the resonance is determined by the intersection of the horizontal line (8) with the $q(B)$ curves.

It is convenient to characterize the position of the resonance by the difference ΔB between the resonance field B_r and the theoretical value of the field of the B_0 of the helicon resonance:

$$\Delta B = B_r - B_0,$$

ΔB is essentially the position of the resonance, reckoned from the theoretical resonant field of the helicon. This quantity can be easily determined experimentally for different frequencies from the positions of the res-
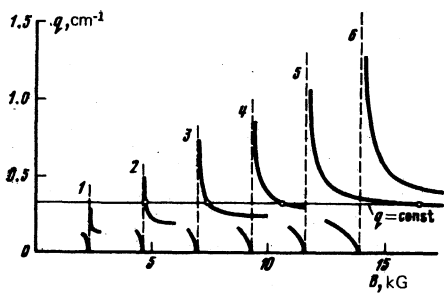
FIG. 5. Dependence of the wave vector of the flexural acoustic waves on the magnetic field in an indium plate 1.5 mm thick at frequencies 22.1, 44.2, 66.3, 88.4, 110.5, and 132.6 Hz (curves 1-6, respectively). The vertical lines correspond to the positions of the helicon resonances at the indicated frequencies. The points of intersection of the curves with the line $q = $ const determines the values of the magnetic fields at which acoustic resonances are produced.

FIG. 7. Positions of observed resonance peaks, reckoned from the magnetic field of the helicon resonance at various excitation frequencies. Points—experimental data, the solid curves were plotted in accord with the theory developed in the present paper.

onant peaks (see Fig. 1).

In the calculation of ΔB, the quantity C in (8) was assumed to be a fit parameter. If it turned out that $CL \ll 1$ (L is the sample length), the calculations were made with the aid of Eq. (7). The plots shown in Fig. 6, which constitute the dependences of the right-hand side of (7) on the magnetic field, were first used to determine the values of J^* and C^* from the positions of the peak at the two frequencies; the same plots could be used next to determine the position of the peak at any excitation frequency.

Figure 7 shows the experimental results and the theoretical curves.

The curves for which $\Delta B > 0$ correspond to excitation, in the plate, of resonances of flexural acoustic oscillations with wavelengths $\lambda = 19.6$, 12.8, and 9.2 cm (curves 1, 2, and 3). The wavelengths were calculated from the values of the fit parameter C. The three cases differed experimentally in the fact that in the first case the sample was placed in the coils and was not glued, in

the second case one end of the sample was glued to the sample holder with BF-2, while in the third case the sample was additionally glued at two other points, approximately 12 mm away from the ends. Obviously, when the number of fastening points is increased and the distance between them is decreased the resonance wavelengths should decrease; this agrees with the character of the change of the fit parameter. The resonance peaks corresponding to the experimental points near the line 4 can be interpreted as ordinary helicon resonances.

Curves 5, 6, 7 correspond to resonant oscillations of the sample holder with the sample fastened to it, varying in the magnetic field in accordance with the condition (7). The peaks closest to the helicon resonance, located on the weak-field side ($\Delta B < 0$, curve 5), correspond to $J^* \approx 1.7 \times 10^3$ g·cm^2 and $C^* \approx 3 \times 10^7$ g·cm^2 sec^{-2}. It follows from this that one of the natural frequencies of the sample holders in the absence of a magnetic field is $f \approx 42$ Hz. Special measurements have confirmed this.

To explain why no splitting of helicon resonances with higher numbers is observed, calculations were made for frequencies corresponding to $n = 1$ and 2 under the resonance condition (2). A typical plot of $q(B)$ in this case is shown in Fig. 8. As seen from the figure, the resonances should occur in fields so close to the heli-
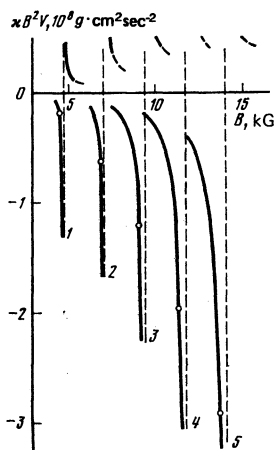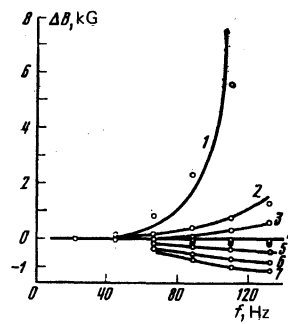
FIG. 6. Dependence of the right-hand side of the resonance condition (7) on the magnetic field at frequencies 44.2, 66.3, 88.4, 110.5, 132.6 Hz (curves 1-5). By way of example are shown the points at which resonances occur at J^* = 1.7 ×10³ g·cm² and C^* = 3 ×10⁷ g. cm² sec⁻².
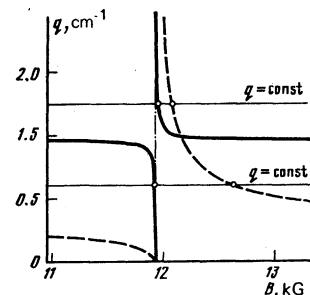
FIG. 8. Example of the dependence of the wave vector q (of flexural waves) on the magnetic field at the frequencies corresponding to excitation of helicon resonance with $n = 0$ in the sample (dashed curves, $f - 110.5$ Hz) and at $n = 1$ (solid curves, $f = 994.5$ Hz). The acoustic resonances occur at the points of intersection of the horizontal lines and the $q(B)$ lines.

con-resonance field, that at the Q factors of the observed resonances these peaks cannot be resolved in the investigated field interval.

Taking into account all the results of the comparison of the theory with the obtained experimental results we can regard the agreement as fully satisfactory. Interest attaches to the extension of the theory to include the case of finite damping of the helicons and of the acoustic oscillations, and also to an investigation of the above-described phenomena under conditions when quantum oscillations of the phase velocity of the electrons set in.[11] These oscillations should lead to quantum oscillations of the characteristics of the acoustic waves.

In conclusion, I am grateful to E. P. Vol'skiĭ, V. F. Gantmakher and V. Ya. Kravchenko for a discussion of the results.

APPENDIX

1. Consider a system consisting of a sample holder, on which is rigidly secured a plate of pure metal, and the holder itself can be rotated through a small angle θ (θ is a vector) lying in the plane of the plate. We assume that this rotation gives rise to elastic moments that obey Hooke's law:

$$G = -C^{*}\theta, \tag{A.1}$$

C^{*} is the elasticity, which we shall assume for simplicity to be a scalar.

In the absence of a magnetic field the equation for the moments takes the form

$$J^{*}\ddot{\theta} = -C^{*}\theta, \tag{A.2}$$

J^{*} is the moment of inertia of the system (which will also be regarded as a scalar) about an axis parallel to the vector θ. Equation (A.2) corresponds to oscillations of frequency ω, defined by the condition

$$J^{*}\omega^{2} - C^{*} = 0. \tag{A.3}$$

In a magnetic field B perpendicular to the plate surface at equilibrium, any rotation of the plate through an angle θ leads to the onset of a tangential component h:

$$h = [B \times \theta]. \tag{A.4}$$

The appearance of the tangential component leads in turn to the production in the plate of a helicon whose field is proportional to h, is directed parallel to the plate surface, and rotates in the same direction as the Larmor rotation of the carriers.[1,2] The entire plate as a unit has in this case a magnetic moment M, which is determined by the value of h and by the helicon characteristics.[3] For the Fourier component M_{ω} we can write

$$M_{\omega} = \varkappa h_{\omega} V, \tag{A.5}$$

$\varkappa$ is the magnetic polarizability,[9] which in the case of absence of helicon damping is a real quantity. V is the volume of the sample.

Allowance for the pondermotive torque $K = M \times B$ acting on the plate leads to the following equation of the moments in the magnetic field:

$$J^{*}\ddot{\theta} = -C^{*}\theta + [M \times B]. \tag{A.6}$$

This equation, with account taken of (A.4) and (A.5),

leads to a new condition for the determination of the resonant frequencies:

$$-\omega^{2}J^{*} + C^{*} = \varkappa B^{2} V. \tag{A.7}$$

2. We consider now flexural acoustic wave in a metal plate, with account taken of the helicon propagation. Assume that the undeformed plate lies in the xy plane and the magnetic field is parallel to the z axis. We derive a dispersion relation for the case when the flexural wave propagates in one direction, parallel to the x axis.

In the absence of an external load, the equation of motion of the length element dx (see Fig. 3) with cross section σ is given by

$$\rho\sigma dx \frac{\partial^{2}u}{\partial t^{2}} = \frac{\partial F}{\partial x} dx, \tag{A.8}$$

where ρ is the density of the metal, F is the force exerted on the element dx by the neighboring elements, and u is the deviation from the equilibrium position.

The torque equation, with account taken of the ponderomotive torque $K = m \times B dx \sigma$, acting on the element dx, where m is the magnetic moment per unit volume of the metal and averaged over the plate thickness, is of the form

$$dx\rho J \frac{\partial^{2}\theta}{\partial t^{2}} = \frac{\partial G}{\partial x} dx + F dx + \sigma[m \times B]_{y} dx, \tag{A.9}$$

where

$$G = EJ \frac{\partial^{2}u}{\partial x^{2}}, \quad J = b \int z^{2} dz, \quad \theta = \frac{\partial u}{\partial x},$$

E is Young's modulus, and b is the width of the plate. Eliminating G and F from (A.8) and (A.9) and neglecting the inertia term in the left-hand side of (A.9), we get

$$\frac{Ed^{2}}{12} \frac{\partial^{4}u}{\partial x^{4}} + \rho \frac{\partial^{2}u}{\partial t^{2}} + \sigma \frac{\partial}{\partial x}[m \times B]_{y} = 0,$$

where d is the sample thickness. Substituting the solution in the form

$$u = u_{0} \exp(-iqx + i\omega t)$$

and recognizing that $m \perp B$, $m_{\omega} = \varkappa h_{\omega}$, $h = B \partial u / \partial x$, we obtain

$$\frac{Ed^{2}}{12} q^{4} - \rho\omega^{2} - \varkappa B^{2} q^{2} = 0.$$

Solving this equation, we obtain the dispersion relation (5):

$$q^{2} = \frac{\varkappa B^{2} \pm (\varkappa^{2} B^{4} + \frac{1}{3}\rho Ed^{2}\omega^{2})^{\frac{1}{2}}}{\frac{1}{6}Ed^{2}},$$

where the plus sign in front of the square root corresponds to the propagating acoustic wave modified in the magnetic field.

[1]E. A. Kaner and V. G. Skobov, Adv. Phys. 17, 607 (1968).
[2]B. F. Maxfield, Am. J. Phys. 37, 241 (1969).
[3]R. G. Chambers and B. K. Jones, Proc. Roy. Soc. (London) A270, 417 (1962). P. A. Penz, J. Appl. Phys. 38, 4047 (1967).
[4]C. Legendy, Phys. Rev. 135, 1713 (1964).
[5]J. R. Merrill and M. T. Taylor, Phys. Rev. 131, 2499 (1963). T. Amundson and P. J. Jestard, J. Phys. F2, 657

(1972).

[6]A. D. Bronnikov, V. S. Dmitrieva, R. K. Nikolaev, and
V. A. Smirnov, in: Metally vysokoĭ chistoty (High Purity
Metals), ed. by Ch. V. Kopetskiĭ, Nauka, 1976, pp. 249–
256.

[7]G. N. Harding and P. C. Thonemann, Proc. Phys. Soc. **85**,
317 (1965). T. Amundsen, *ibid.* **88**, 757 (1966).

[8]J. A. Delaney and A. B. Pippard, J. Phys. **C4**, 435 (1971).

[9]L. D. Landau and E. M. Lifshitz, Élektrodinamika sploshnykh
sred (Electrodynamics of Continuous Media), Gostekhizdat,

1957 lPergamon, 1959].

[10]E. Skudrzyk, Simple and Complex Vibratory Systems, Penn.
State Univ. Press.

[11]E. P. Vol'skii and V. T. Petrashov, Pis'ma Zh. Eksp.
Teor. Fiz. **7**, 427 (1968) [JETP Lett. **7**, 335 (1968)]; Zh.
Eksp. Teor. Fiz. **59**, 96 (1970) [Sov. Phys. JETP **32**, 55
(1971)].

Translated by J. G. Adashko

Effect of linear defects on the local magnetization of a plane Ising lattice

R. Z. Bariev

Kazan' Physicotechnical Institute, USSR Academy of Sciences
(Submitted 12 April 1979)
Zh. Eksp. Teor. Fiz. **77**, 1217–1229 (September 1979)

An exact solution is obtained for the local magnetization of a plane Ising lattice with a line of defects of
two types. It is shown that near the critical point, at distances to the defect much shorter than the
correlation radius, the local magnetization has a universal behavior that manifests itself in the fact that
its critical exponent is a continuous function of the microscopic parameters of the system.

PACS numbers: 75.10.Hk, 61.70.Ph

1. INTRODUCTION

The study of the influence of various defects on the
critical behavior of systems that undergo phase transi-
tions is of condiserable influence both theoretically and
experimentally. The theoretical study of this influence
is based on phenomenological theories,[1-5] renormaliza-
tion-group calculations,[6,7] high-temperature expansions
as well as on exactly solvable models.[1,11-14] Principal
attention is being paid to the study of the influence of the
defects on the global characteristics of the system,
such as the transition temperature, the free energy, the
specific heat, etc. No less interesting, however, is the
study of the influence of the defects on local character-
istics such as the local magnetization and the correla-
tion functions. The reason is, first, that the influence
of the defects on the local characteristics is stronger
than on the global ones, and second, that in a number
of experiments it is precisely the local characteristics
that are measured.

This paper presents a rigorous analysis of the influ-
ence of linear defects of two different types on the local
magnetization of a plane Ising lattice. Fragments of the
lattices considered are shown in Fig. 1. The local
magnetization is calculated exactly for these models,
and a study is made of its dependence on the distance
to the defect and on the size of the defect. The most in-
teresting feature of the solution is the dependence of the
critical exponent of the local magnetization on the in-
teraction parameters.

The systems considered simulate real objects in

which the defects are due to the presence of one dislo-
cation. They constitute the linear approximation in the
analysis of objects having a low dislocation density.

2. FORMULATION OF PROBLEM

The interaction energy of the considered lattices can
be represented as a sum of two terms

$$E = E_0 + \Delta E, \tag{1}$$

where E_0 is the energy of the interaction of the defect-
free lattice:

$$E_0 = -\sum_{m=1-M}^{M} \sum_{n=1-N}^{N} (J_1 s_{mn} s_{m,n+1} + J_2 s_{mn} s_{m+1,n}), \tag{2}$$

ΔE is the energy of the perturbation due to the presence
of the defects. For the lattice of the first type

$$\Delta E = -(J_1' - J_1) \sum_{m=1-M}^{M} s_{m0} s_{m1}, \tag{3}$$
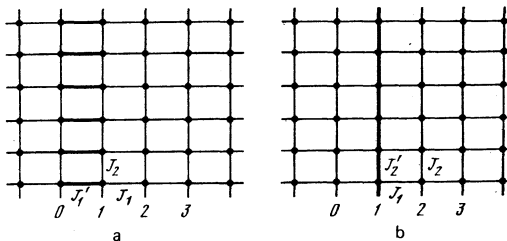

FIG. 1. Fragments of plane lattice with line of defects located
between two neighboring columns (a) and inside one column (b).